







High nitrous oxide emissions from temporary flooded depressions within croplands

By Bo Elberling ¹✉, Gyula M. Kovács¹, Hans Frederik E. Hansen¹, Rasmus Fensholt ¹, Per Ambus ¹, Xiaoye Tong¹, Dimitri Gominski¹, Carsten W. Mueller ^{1,2}, Daniel M. N. Poultney ¹ & Stefan Oehmcke ³

Nitrous oxide is an important greenhouse gas and emissions from managed ecosystems are directly correlated to anthropogenic nitrogen input. Here we have measured nitrous oxide emissions from flooded depressions within croplands and from incubated soil samples. We scaled emissions to >20,000 comparable flooded depressions across Zealand in Denmark using a deep-learning approach based on aerial photos and satellite images. We show that flooded depressions within cultivated fields, representing less than 1% of the total cultivated area, can release 80 times more nitrous oxide compared to rest of the fields. Fluxes can remain high for more than two months after fertilisation and can account for $30 \pm 1\%$ of the nitrous oxide budget during that period. This highlights the urgent need for assessment of nitrous oxide hotspots, as managing these hotspots appear to represent an important part of the overall greenhouse gas emissions from managed croplands and an efficient mitigation action.

¹Department of Geosciences and Natural Resource Management, University of Copenhagen, Øster Voldgade 10, 1350 Copenhagen K., Denmark. ²Institute of Ecology, Technische Universität Berlin, Ernst-Reuter-Platz 1, 10587 Berlin, Germany. ³Department of Computer Science, DIKU, University of Copenhagen, Universitetsparken 1, DK-2100 Copenhagen Ø, Denmark. ✉email: be@ign.ku.dk

Nitrous oxide (N_2O) is considered the third most important greenhouse gas after carbon dioxide (CO_2) and methane with a global warming potential 298 times that of CO_2 over a 100-year timespan¹. Agricultural N_2O emissions resulting from manure and nitrogen-based fertilisers have dominated global anthropogenic N_2O emissions for decades^{2–4}. Emissions of N_2O are a consequence of nitrogen (N) inputs to soil and occur via a range of microbial transformation pathways including nitrification, nitrifier-denitrification and denitrification⁴. Oxygen availability is a key determinant of these N_2O producing processes⁵. Under oxic conditions, nitrification converts ammonia to hydroxylamine, nitric oxide, nitrite and nitrate, and N_2O is produced as a result of abiotic or biotic transformations of the intermediates^{6,7}. The process of NO_3^- reduction via denitrification occurs under anoxic conditions, where N_2O is an obligate intermediate in the denitrification pathway.

Temporal and spatial variability challenge our understanding of N_2O emissions, particularly in relation to hotspots (or short periods known as hot moments) to explain high emissions^{8,9}. We consider croplands that become temporarily flooded as a potential hotspot for fast denitrification process, resulting in a relatively large fraction of N being converted quickly to N_2O . “Hot moments” have been shown to be the case in relation to drought followed by rewetting for managed grassland⁶ and in depressions within the first four weeks of spring thaw⁷. We consider the period immediately following fertilization as a potential hot moment, particularly if nutrient-rich near-surface water quickly can reach flooded depressions, which therefore may become hotspots. The next steps to quantify the importance of flooded fields include: (1) to quantify the order of magnitude in N_2O emissions from flooded depressions within contrasting fields, (2) to quantify the duration of high N_2O fluxes from such depressions and finally (3) to quantify the area-contribution of such depressions within a larger region. These three targets have all been addressed in this study. Here, we focus on the distribution and role of field hotspots for N_2O emission associated with spring fertilization.

Denmark has relatively flat croplands with rolling hills shaped by past glaciers and water and dominated by intensive farming¹⁰. It has enough topography to form gradients for surface or near-surface water to flow towards depressions within individual fields⁹. Despite the spatial variation in elevation, fields receive the same order of magnitude of N from fertilization. That means that water with high concentrations of inorganic N (mainly nitrate) can accumulate in poorly drained areas^{11,12}, which typically become flooded annually during winter and spring. Small-scale depressions and flooded fields have not been included in current national greenhouse gas budgets¹¹ despite cultivated soils generally have been identified as potential source areas for high N_2O fluxes particularly related to early spring fertilisation prior to the main growing season^{12–14}. Recently, N_2O emission hotspots at plot and landscape scale have been associated with organic soils under warm well-drained conditions¹⁵. This study aims to assess this knowledge gap by quantifying the area and duration of flooded mineral soils within intensively managed croplands combined with detailed in-situ N_2O flux measurements of both flooded and non-flooded areas within fields as well as N_2O flux measurements under controlled laboratory incubations.

Results and discussion

In total 102 partly flooded fields (from less than 0.4 to 2.5 ha) have been identified within a 9000 km² area in the central part of Zealand in East Denmark in 2018 and 2019 (see area marked in red in Fig. 1). Subsequently, the entire island of Zealand was surveyed to identify the number and area of similar flooded fields

for the period March–April 2019. For that we used a deep-learning approach to identify and segment single ephemeral water bodies in remotely sensed images at 3-m spatial resolution (Fig. 1).

Due to the dispersed emergence of ephemeral water bodies on cultivated land, their appearances/shapes could be distinguished based on a deep learning segmentation and a combination of optical and topographic remotely sensed information, due to the markedly different appearance from their surrounding cropland areas that are largely uniform in spectral properties and appearance (see “Methods” for detailed description). In total 20,063 individual flooded areas within fields were identified with an average size (\pm one std) of 802 ± 150 m² and in total equal to 23.1 ± 1.3 km². That means that flooded areas within fields represent 0.50% of the total farmed area of Zealand equal to 4,973 km². Of these flooded areas, the rim area (5 m rim of each flooded area) represented 0.26% of the farmed area (and equals 13.2 ± 0.8 km²), which in the following is considered a key hotspot for N_2O emissions. See Table S1 for accuracy metrics.

The duration of flooding during the two-month study period of March/April 2019 was assessed by mapping the near surface wetness index (see methods and supplementary Figs. 1, 2) and indicated that individual flooded depressions within fields varied in size but that the area-integrated area being flooded over the two months did not change significantly. This is consistent with the general pattern observed in the field.

Spring N_2O bursts. During spring 2018/2019 after fertilisation, fluxes of N_2O were measured once at 102 different flooded fields including measurements in the central part of the flooded area, at the rim of the flooded area and at drained adjacent locations representing a background value for N_2O characterising the remaining part of the field (each location in 3 replicates). This measurement campaign is considered a snapshot of the spatial variability of N_2O fluxes measured within two months after fertilisation and prior to the main growing season (regardless of main crop and time since fertilization). Flux measurements were made using static chambers and by measuring the N_2O concentrations for 12 min in each chamber with a photo-acoustic gas monitor (INNOVA 1312, Lumasense Inc., Ballerup, Denmark)¹⁶. Flux measurements were accompanied by soil temperature and soil moisture measurements as well as soil samples taken for soil pH measurements and nitrate analysis. See details under “Methods”.

N_2O emissions in the rim area of the flooded area (the rim defined as being completely saturated and without standing water of more than 0–1 cm) were significantly higher compared to any other part of the fields (Fig. 2). Emission rates in the centre of the flooded depression remained generally lower but emitted highly variable amounts of N_2O compared to the upland parts of the fields. On average, N_2O fluxes from the rim area of the depressions were 652 ± 118 $\mu\text{g N m}^{-2} \text{ h}^{-1}$, corresponding to more than 80 times higher average N_2O flux than at adjacent locations (8 ± 2 $\mu\text{g N m}^{-2} \text{ h}^{-1}$). The latter value was consistent with previous numbers reported from Denmark^{11,17–19}. The N_2O fluxes corresponded to soil temperatures between 2–7 °C and a mean soil pH of 6.4 ± 0.3 without significant differences between flooded and non-flooded parts of the fields. Soil moisture measurements for the centre and the rim of flooded fields revealed complete water saturation and water contents by volume varied between 45 and 52% corresponding to the soil porosity. For adjacent locations, the soil water content was in average $32 \pm 8.3\%$ by volume. Corresponding nitrate concentrations revealed a significant and positive correlation of high fluxes and high concentrations of nitrate in the rim area (see Supplementary Fig. 4).

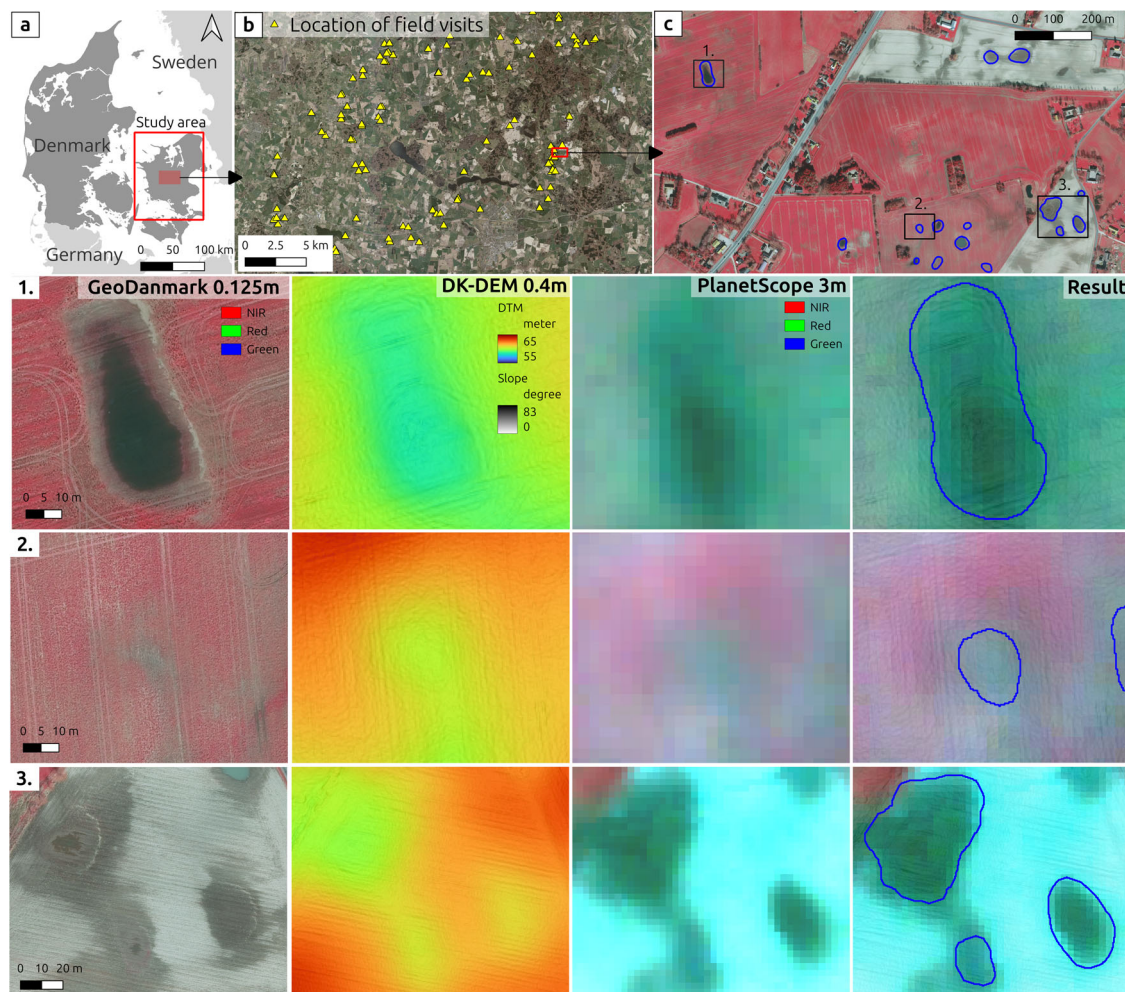


Fig. 1 Examples of flooded fields in the study area Zealand in Denmark. **a** Total study area Zealand in Denmark, the study area of 102 flooded depressions is marked as a red square and shown in detail in **(b)**. **c** 1–3: Examples of flooded fields with various contrast and background conditions as they appear at various spatial resolutions, showing the resulting segmented boundaries.

Laboratory fertilisation experiment. During the autumn 2022, a sensitivity test was made based on intact soil cores collected from a typical loamy soil from one of the adjacent locations to a flooded field. A water and nitrate addition experiment was made simulating three water content levels (freely drained, ambient and total flooded conditions) with nitrate addition in three treatments: low (10 kg ha^{-1}), normal fertilisation level (50 kg ha^{-1})²⁰ and triple fertilisation level (150 kg ha^{-1}). The treatments corresponded to an addition of 3.8, 19.2 and 57.7 mg N as nitrate per core. The latter level is made to mimic split fertilisation practises²⁰, which is commonly applied in the area and/or the fact that fertilisation near flooded fields is high as tracks in many cases (based on aerial photos, supplementary Figure 3) show that machineries are driving around rather than through flooded areas of fields. All treatments were made in three replicates; in total 27 cores were pre-incubated for 2 weeks and subsequently incubated at 7°C for 75 days. N_2O emissions were measured using an Isotopic N_2O Analyzer (914-0027 from Los Gatos Research, Quebec, Canada).

Mean laboratory fluxes (Table 1) show that under normal fertilisation rates of nitrate, field and laboratory observations under completely flooded conditions are in the same order of magnitude; around $400 \mu\text{g N}_2\text{O-N m}^{-2} \text{ h}^{-1}$. Field measurements are higher, which is in line with the fact that soil cores in the incubation represent emissions from N_2O produced and released from the top 12 cm of the ploughing layer only. In contrast,

measurements in the fields represent N_2O produced and released from the entire soil profile; presumably from the top 30 cm mainly, representing the ploughing layer.

The results (Table 1) illustrate that the very same soil can release from 0.7 to $1072 \mu\text{g N}$ as N_2O per m^2 as a mean over 8 weeks only reflecting the nitrate input and the environmental conditions in terms of drainage/flooding. For a “normal” nitrate addition, the flooded cores released on average 370 times more N_2O as compared to ambient conditions, while under “high” nitrate addition the flooded cores released 29 times more N_2O as compared to ambient conditions and 536 times as compared to dry conditions. These incubation-based values can be compared to the factor of 80 observed under field measurements, which indeed is in the low end of the increased rate due to flooding. Other soil characteristics measured ($\pm \text{st. dev}$) show that the bulk density was $1.4 \pm 0.1 \text{ g cm}^{-3}$, the soil organic carbon content was $1.59 (\pm 0.09)\%$ and the nitrogen content was $0.18 (\pm 0.01)\%$. The average C:N ratio was 8.85 and soil pH was $6.25 (\pm 0.03)$. These soil characteristics indicate that it is a common cultivated soil in Zealand²¹, which can be considered a Luvisol representing a soil type covering more than 95% of the area in Zealand²¹.

Landscape integrated N_2O fluxes. The importance of N_2O hot-spots in regards to greenhouse gas mitigation is on the agenda in

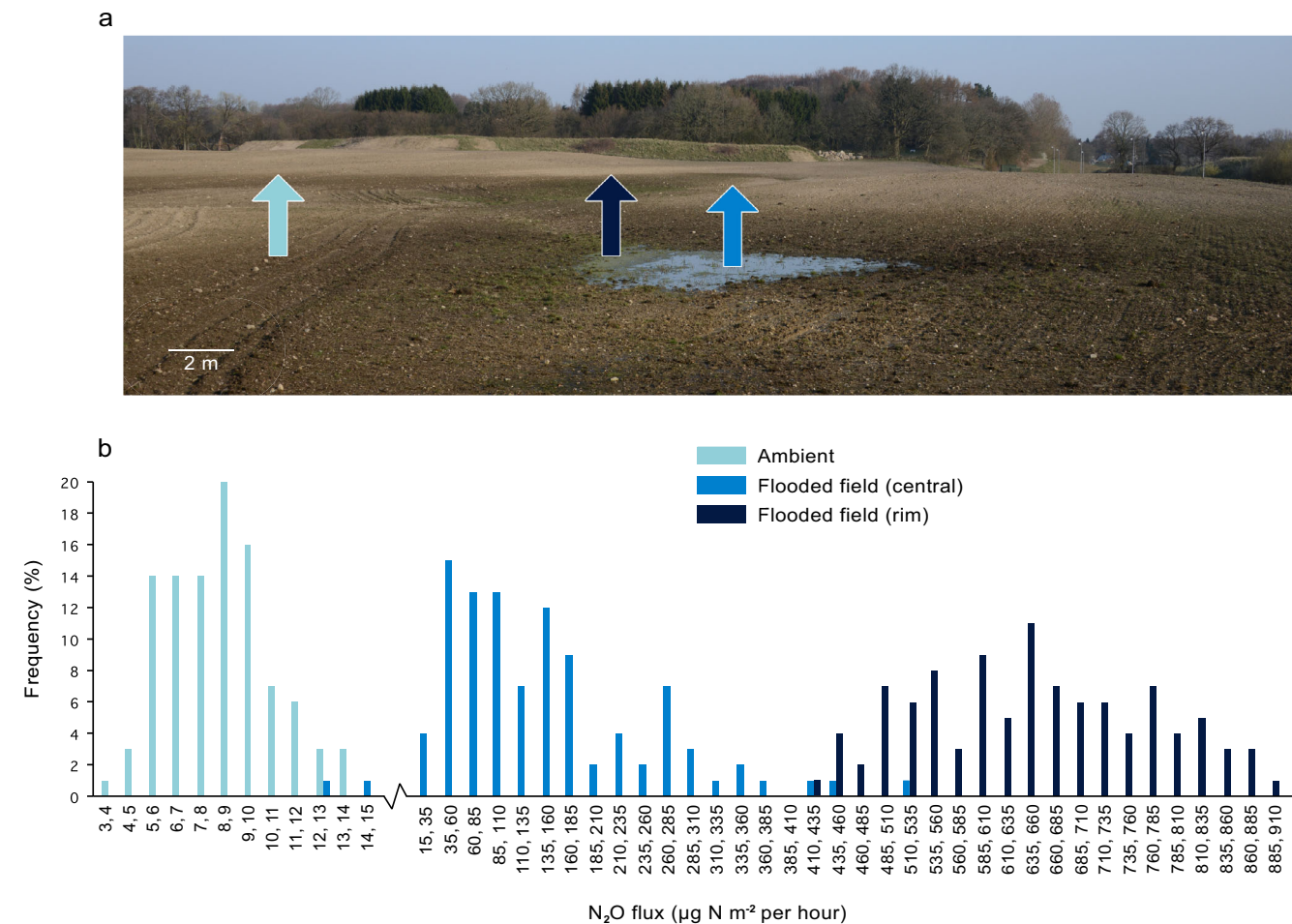


Fig. 2 The frequency of N₂O fluxes measured at three categories of fields. **a** Example of a flooded field, which for the particular field represents about 0.2% of the entire field equal to the mean across Zealand during intensive fertilisation in March/April. **b** Histogram showing the frequency of mean N₂O fluxes measured at three categories of fields: the central part of the flooded field with standing water, the rim area of the flooded part and the ambient field surrounding the flooded part.

Table 1 Mean fluxes in µg N ₂ O-N m ⁻² h ⁻¹ (standard deviations given in brackets) for the eight weeks of the laboratory experiment for three nitrogen levels (Low = 10 kg ha ⁻¹ , Normal = 50 kg ha ⁻¹ and High = 150 kg ha ⁻¹).			
	Low	Normal	High
Drained	1.7 (5.3)	0.7 (2.8)	2.2 (6.4)
Ambient	24.7 (74.7)	1.1 (2.9)	37.6 (129)
Flooded	66.3 (114)	410.1 (295.3)	1,072.2 (633.8)

See Supplementary Table 1 for mean fluxes and emission factors after one, two and eight weeks, respectively.

most countries with intensive farming^{12–15}. Thus, scaling the above results to a larger area as Zealand is important for assessing the wider significance of this phenomenon, but is also related to sources of uncertainty. Consequently, we here present a conservative estimate based on the following discussion and criteria's:

1. The study period (2018/2019) was relatively normal in terms of precipitation. However, both years reflect an increasing tendency of warmer summers (particularly the summer 2018) and less precipitation during the main growing season and more episodic precipitation events during autumn²².
2. We assume that the 102 fields represent an average in relation to land use practice, although they cover a range of fields depending on crop types, crop rotation, specific farmer fertilisation strategies etc. Many of these variables will vary from year to year but will typically do so within a four-year cycle. Thus, snapshot measurements of 102 flooded fields show that a typical agricultural soil in Zealand in Denmark can release 80 (during incubation up to 140) times more N₂O solely depending on nitrate availability if kept under completely water-saturated conditions.
3. Field measurements were completed within a two-month period which equal the period where flooding was observed. The duration of flooding was verified based on an assessment of a near-surface moisture index as derived from (see supplementary figure 1). From this we consider the snapshot measurements of 102 lakes to represent a mean flux across two months. This is further justified by the incubation experiment revealing high fluxes for at least 8 weeks after nitrogen addition (Fig. 3).
4. We have identified 20,063 similar partly flooded fields across Zealand. We assume that N₂O emissions from the 102 flooded areas within fields are representative for the 20,063 flooded areas across croplands in Zealand. This is justified by the overall variation and mean value of soil development and soil characteristics (including nitrate

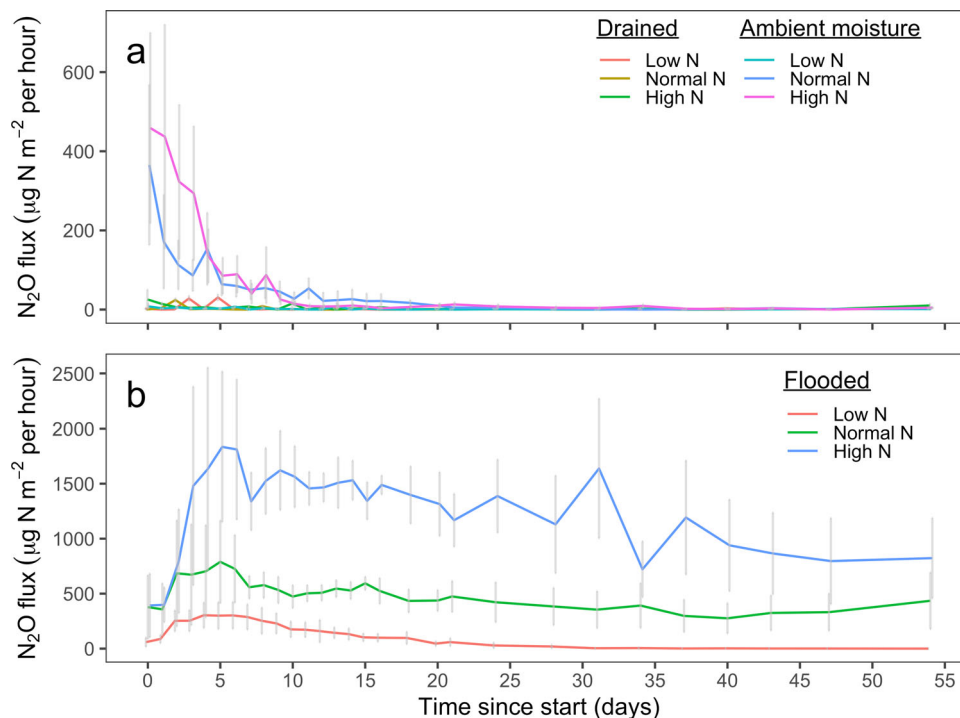


Fig. 3 Measurements of N₂O fluxes for 74 days during incubation experiment. Daily measurements of N₂O fluxes for the first 17 days and less frequently afterwards for (a): drained, ambient and (b): flooded conditions (standard errors are shown as bars). Please see Supplementary Fig. 5 for details for all three soil moisture levels.

concentrations, soil pH, %C and C/N) from the 102 fields and soil maps covering Zealand and the area representing the 102 flooded areas.

Scaling these results to a larger area as Zealand; considering (1) flooded fields during a two-month period, (2) only the 5-m rim of flooded fields and (3) an average rate of N₂O emissions being 80 times higher as compared to the rest of the field, we conclude that these hotspots represent $30 \pm 1\%$ of the total N₂O emission during that period. The uncertainty range refer solely to the uncertainties related to the area estimates of flooded fields (see Fig. S2). We consider the 30% being a minimum value, which is most likely markedly higher. Factoring in the entire flooded area (and not only the 5-m rim area) will increase the percentage of N₂O emission from flooded fields, however, results presented also reveal a larger variability in fluxes if the entire flooded area would be included.

The results also highlight that the total area of flooded area within fields is not a suitable measure to estimate the total N₂O loss, as a strong gradient in emissions may appear along the topography near flooded fields. The extremely high N₂O fluxes are measured at the rim of the depressions (presumably partly due to receiving water from uphill soils) whereas lower fluxes are measured in the central part of the depressions. These lower fluxes measured in the central part may point at that nitrate reduction at the rim is fast and that water is depleted with respect to nitrate before reaching the central parts of the depressions and that nitrate from deeper sources (groundwater) is less important for the observed high N₂O fluxes. The depression size-dependency and scaling of N₂O fluxes across fields with e.g., different soil types, crops and management strategies are some of the most important unknowns in order to estimate the environmental and economic loss of N₂O (and nitrogen) in depressions.

In general, main factors controlling the formation of hot moments of N losses have been identified to be temperature, precipitation and fertilisation. Roy et al. (2021)¹³ concluded,

based on a US country-level assessment on nitrogen budgets, that a variety of hot moments and hotspots collectively may account for about 63% of the total surplus nitrogen balance. The nitrogen loss as N₂O was part of the budget, but not specifically quantified due to lack of hotspot measurements¹³. Wallman et al. (2022)¹⁵ measured N₂O emissions related to fertiliser treatments and observed extreme N₂O bursts associated with the actual fertilisation. However, the study did neither include measurements under anaerobic conditions or lateral movement of fertiliser across the field. Wagner-Riddle et al. (2020)¹⁹ specifically included hotspots and hot moments (fertilisation events) as part of recent review of mitigation actions to minimise nitrogen emissions from agroecosystems. Kim et al. (2013)²³ made a meta-analysis showing a strong dependency of N₂O emissions on soil nitrogen availability which is aligned with our field observations. They showed that N₂O emissions increased linearly with increased N input in the range of 10–150 kg N per ha, but also that N₂O emissions increased non-linearly (almost exponentially) with N inputs larger than 150 Kg N. Del Grosso et al. (2022)²⁴ used an ecosystem model to quantify how land management practices and weather can control nitrous oxide emissions. They concluded that spring-thaw-related N₂O pulses in northern agroecosystem regions of the United States occur for a short period, but increase the emissions from croplands and grasslands by up to 16% at the national level.

The above mentioned references clearly demonstrate a growing awareness of hotspots (and hot moments) being critical and important for robust N budgets for croplands, but also that hotspots, as flooded depressions within fields, remain a major knowledge gap which need to better understood and quantified in order to improve mitigation actions and optimise the use of fertiliser. We conclude that the extreme importance of a relatively small area within field for area-integrated N₂O emissions is completely new in literature and suggests an urgent need to address management of these hotspots.

Our study focuses on the end of the non-growing season/start of the growing season. However, the non-growing season has recently been shown to account for 38–43% of the annual N_2O emissions depending on crop type based on a study of Canadian croplands²⁵. Taking the conclusions from the present study may markedly increase the importance of the non-growing season and the transition to the growing season. The same study²⁵ also showed that the percentage of added N released as N_2O (the emission factor) varied from 0.29–7.32% for yearly emissions but only 0.12–2.02% for the growing season. Our experimental incubation suggests that more than 5–8% of added nitrate is being released as N_2O to the atmosphere (see Supplementary Table 1). Such high emission factors stand in contrast to the commonly accepted factor of 1% used in national greenhouse gas inventories (NGGI)¹¹. However, due the limited area of flooding (less than 1%), results presented here cannot be used to argue that the currently used emission factor based on an average for individual fields needs to be adjusted. In addition, despite the focus on the non-growing season as crops start to grow, plants will compete with microorganisms for N and thereby reduce the N_2O production. Finally, incubation experiments are excellent for keeping environmental factors constant during measurement campaigns, but more sites representing different soil types, climate and management practice are important to reduce uncertainty before scaling our numbers to national or larger region N_2O budgets. This is relevant in the light of only one soil type being included in the incubation experiment. Although a representative site and soil type in terms of soil characteristics has been chosen for the incubation experiment, variations in soil type are expected to have consequences for observed N_2O fluxes and the overall N_2O budget. Similarly, we have in this study focused on an actual time period (an actual year and spring time only), but year to year variations can be critical for both the area within field being flooded, but also the time period being flooded, and also the environmental conditions while flooded. Particularly, soil temperature, precipitation events and nitrate availability while flooded are expected to impact the net N_2O budget for flooded fields.

Implications and recommendations. Due to gravity, even minor depressions are the final destination for water runoff from surrounding upland fields, with reduced infiltration rates and longer residence times of water compared to the upland areas. This means that they are more prone to being waterlogged and becoming anoxic, particularly in the non-growing season. Hydrological models and continuous measurements of nitrate are needed to identify: (1) the upland areas, (2) runoff patterns towards depressions (runoff versus groundwater) and (3) the residence time of water and nitrate in depressions.

Large precipitation events (producing waterlogged areas or floods) occur mainly during the non-growing season. They are a result of cyclic patterns and are considered to increase in frequency and intensity in the future²⁶. In relation to N_2O hot moments, early spring fertilisation events are considered very critical. A similar hot moment is likely after the “first precipitation event” following a prolonged drought²⁷. This is a typical autumn situation, where the timing and intensity of rain will determine how much nitrate is being flushed out from the part of the field surrounding the depressions^{28,29}. Currently, there are no estimates of the overall proportion of nitrate in fields that can be mobilised and potentially transported to depressions and subsequently converted to N_2O and free nitrogen (N_2) by denitrifying microorganisms. It is important to note, that in contrast to N_2O , the release of N_2 is not an issue for the climate. But any loss of nitrogen represents a loss of resources seen from a

farming perspective. This is also the case in paddy soils where high fluxes have been measured after soil drainage³⁰ but here nitrification is considered the main process as a source of N_2O . Without a loss, the nitrogen pool would otherwise have been kept in the soil system and increased growth and crop yields in the following growing season.

Thus, N_2O hotspots are an essential focus point for planning actions to reduce the overall greenhouse gas footprint of the agricultural sector. Currently, N_2O hotspots are not included in national N_2O budgets¹¹. The lack of measurements is likely the main reason for this avoidance, probably reflecting the logistical problems of obtaining solid N_2O flux measurements with flux chambers in muddy/flooded fields. The results shown here suggest that nitrate pulses and associated N_2O bursts can have a duration of days to several weeks, which highlights that high-temporal measurements are necessary to capture the N_2O bursts. This has also been proven in wetland ecosystems⁵ and the technology for implementing similar setups in cultivated fields is available.

Policies for taking cultivated land out of production in order to reduce net greenhouse gas emissions, as a means for securing a successful green transition, are on the political agenda right now. In many regions, farmers and environmentalists agree that a promising option to reduce net greenhouse gas emissions is to convert existing croplands to nature. This agreement between farmers and environmentalists is based on a willingness of spending public money to cover some of the cost for such land use changes. Therefore, the critical question is which part of the cropland should be converted in order to obtain the highest benefits for the climate, nature and farmers. From a farmer's perspective, the periodically flooded fields are often considered the least cost-effective to operate, least accessible (part of the time), most in need of re-sowing, and, despite the hassle, usually supplying no or low yields. Consequently, flooded areas within fields appear to be giant N_2O emitters and represent a low hanging fruit in relation to greenhouse gas mitigation actions.

We conclude that fluxes of N_2O in and near flooded depressions within fields are extremely high when nitrate levels are high (particularly after fertilisation) and fluxes in the rim area of flooded fields are 80–140 times higher compared to similar soil types being effectively drained. Fertilisation (which is often repeated during springtime) can be considered a hot moment and flooded fields an example of extreme hotspot, showing very high nitrate values and corresponding extremely high N_2O emission for at least 8 weeks. During such conditions, laboratory results suggest that more than 5–8% of added nitrate is being released as N_2O to the atmosphere. Flooded depressions within fields are found widespread in Zealand but represent only an area of less than 1%. Scaling these field-measured fluxes to Zealand in Denmark show that during a two-month period, the rim area of flooded fields representing 0.26% of the farmed land can release 30% of the total N_2O emission. Consequently, land use changes taking flooding of fields into account are very likely a strong win-win opportunity for climate, nature and farmers.

Methods

Mapping flooded fields. This study demonstrates a framework for mapping ephemeral water bodies in surface depressions of agricultural fields with satellite imagery at very high spatial and temporal resolution. This combination of rich information in both space and time, which is otherwise not feasibly achievable from common freely available satellite remote sensing systems, is obtained from the use of the constellation of 130 nano-satellites from the Planet company. We trained a deep convolutional network with the widely used U-Net architecture^{31,32} for

semantic segmentation to predict pixel-wise ephemeral water body coverage on remotely sensed PlanetScope images at 3-m spatial resolution supported by a detailed (40 cm) LiDAR-based DEM (digital elevation model). We expected the fusion of optical and elevation data to help discriminating water bodies from their surroundings.

Therefore, we devised a strategy based on a set of rules to identify ephemeral water bodies in satellite images -, according to which we manually delineated and annotated 1824 individual objects across Zealand that were verified using very high-resolution nationwide aerial photography provided by the Danish Agency for Data Supply and Infrastructure (SDFI). These orthophotos were collected at 12.5 cm spatial resolution as a patchwork of 4-channel RGBNir images varying between 29 March – 18 April, which despite being useful for supporting visual assessment during the training data collection, lack the temporal consistency for large-scale analysis. We ensured that the labels represent a wide range of landscape characteristics, by defining and balancing five subcategories depending on how water and vegetation are spatially distributed. The collected water bodies showed a distinct visual contrast and a clear surface depression corresponding to the object coverage, which excludes surfaces with soil saturation without notable topographic variation. In addition, we only labelled objects that showed a high temporal variability that we visually assessed in very high-resolution aerial photography covering a period of seven years, as well as based on the presence of permanent vegetation, such as trees, shrubs, or emergent plant types, which we excluded from the delineation. The manually labelled water bodies were used to train and validate the deep-learning model, which was then used to predict ephemeral water bodies covering the whole study area.

The input features given to the deep learning model were PlanetScope level 3B Ortho Tile imagery at a 3-m spatial resolution and daily temporal resolution that consists of three visible (VIS: 0.40–0.75 μm) and one near-infrared (NIR: 0.75–1.30 μm) bands with a maximum of 20% cloud cover (Fig. 1). We selected a three-week temporal window from 29 March to 18 April to compose our median PlanetScope mosaic with an average of 36 cloudless mosaics for each 25-km x 25-km tile after cloud removal. This period corresponds to an observed peak in the water signal, which is useful to maximise the contrast between the ephemeral water bodies and their surrounding cropland, and minimise noise from occasional snow cover.

We obtained the temporal dynamics of the ephemeral water bodies using six months of PlanetScope data over 102 field-collected sites that showed a high intra-annual variability (Fig S1), with a strong peak during March and April, followed by a sudden decrease - in contrast to permanent small water bodies that displayed a more stable trajectory. We used a single band thresholding technique of the NIR band to calculate the water fraction (WF), based on the bimodal distribution function representing reflectances over water and land surfaces. The water and land limit thresholds (WL: 1300 and LL: 4500) were empirically identified to separate the pure water and land signals from the mixed pixels, as $\text{WF}(\%) = (\text{LL} - \text{NIR}) \times 100 / (\text{LL} - \text{WL})$ ³¹. We calculated the temporal variability from all >80% cloud-free daily data using a 5-day median between January and July 2019.

We supplemented our PlanetScope composites with data from the Danish Elevation Model (DK-DEM) at a 0.4 m resolution showing elevation in relation to the average sea level (Fig. 1), which is based on 415 billion points covering the entire country, collected by aerial LiDAR and is provided by the Danish Agency for Data Supply and Infrastructure (SDFI). We included a digital Terrain Model (DTM), a Digital Surface Model (DSM), and a DTM-derived slope layer. The DSM contains information about the height of surface objects, such as vegetation or buildings in

relation to mean sea level, which are removed from the DTM. We hypothesized that information about differences in terrain and surface object height can be useful in differentiating areas of low reflectance, such as shadows that are other than ephemeral water bodies.

The deep-learning model was trained with gradient descent using a learning rate of 0.0003 and an adaptive learning rate optimization algorithm (Adam), which computes separate learning rates for each parameter³³. We employed the cross-entropy loss function during the 500 epochs of training with a batch size of 16, a patch size of 256, along with batch normalization³⁴ and using rectified linear units (ReLU) as the activation function³⁵. To increase the variability of the dataset, we augmented the training data with artificial and transformed training images (e.g. vertical flip, horizontal flip, rotation, gaussian noise, pixel dropout)³⁶. After each epoch, the model was evaluated on an independent validation set (20% of the labels) and we selected the final model with the lowest validation loss value of 0.5670. The predicted map conveys the location of each detected ephemeral water body and its area coverage in m^2 .

After the prediction, we used morphological filtering with a 6x6 structuring element to eliminate noise resulting from image artefacts and edge effects, and to smoothen the occasionally fuzzy object boundaries caused by low contrast conditions. We used the independent validation set to calculate the prediction accuracy of the filtered product (Fig. S”). The total accuracy of predicting water body pixels was 72%, the balanced total accuracy of background as well as water body pixels was 86%, and the precision of predicting water body pixels was 50% (Table S1). Additionally, we used the derived error rates to proportionally adjust our area estimates and calculate their 95% confidence intervals³⁷. Ephemeral water bodies represent areas being a continuum from flooded fields to wet soils. Given the nature of ephemeral water bodies, where no exact borders can be drawn between target and background in relation to the spatial extent, the pixel-based accuracy obtained is considered satisfactory. At instance level, we report 34% precision and 34% recall (34% F-score) when associating predicted and labelled individual water bodies with a minimum intersection over union (IoU) of 20%. The true positives have an average IoU of 46% with their corresponding labelled objects. Additionally, we report an overall water body counting error of only 3% on the validation set (216 labelled objects, 223 predicted), showing that the model has a good balance between false positives and false negatives. The post-processed results became the basis for calculating the total area coverage, as well as estimating the area under the rim-effect using a 5-m buffer from each object outline, as established by observations from the field.

The uncertainty of mapping ephemeral water bodies in general, and with a coverage of <150 m^2 in particular, is comparatively high, because of their dynamic nature, as they may emerge after a rainfall event but are often rapidly drained away afterwards. This can cause a variation within image composites using different dates, which is inherent to the use of very high-resolution satellite image analysis for regional scale analysis. An additional source of potential inaccuracy is caused by relatively large fields that are uniformly wet or show a wet, narrow swath along the field boundary, creating contrast conditions that are suboptimal for accurate detection.

N₂O flux measurements. In situ fluxes of N₂O were measured along transects at each flooded area within fields and after the first fertilisation event (in March). The general strategy for farmers is to fertilise first time when possible followed by two more intense fertilisation events at the end of March or start of

April. The typical total load of N is 150–200 kg N for these three fertilisation events. The main growing season is considered from mid April. The high number of sites in this study reflects the focus on robust mean values rather than replicates reflecting crop type, time since fertilisation or general management practices. Sites were consequently selected randomly within the study area.

At each of the 102 locations, N₂O fluxes were measured at three positions along a transect (centre, rim and upslope) in three replicates. Flux chambers made of PVC tubes (diameter of 24 cm, height of 20 cm) were inserted 2 cm into the soil. Flux measurements were made by placing a lid on the tube and measuring the N₂O concentration for 12 min in each chamber with a photo-acoustic gas monitor (INNOVA 1312, Lumasense Inc., Ballerup, Denmark). The closed-chamber technique is known to create a bias by altering the diffusion gradient between soil and chamber headspace (Livingston and Hutchinson, 1995). However, several studies have shown that this bias can be overcome by applying a non-linear regression method to describe the gas exchange (Forbrich et al. 2010). In our case, the flux in each chamber was estimated by fitting the increase in N₂O concentrations to a nonlinear function for measurements starting 2 min after the lid was placed. For N₂O flux calculations, concentrations of N₂O were converted from ppm to $\mu\text{mol m}^{-3}$ using the ideal gas equation and subsequently the flux was estimated using:

$$F = dC/dt \times V/A \quad (1)$$

where F is the N₂O flux ($\mu\text{mol m}^{-2} \text{hour}^{-1}$), C is the concentration of N₂O ($\mu\text{mol m}^{-3}$), t is time (hours), V is the volume (m^3) and A is the area of the soil cylinder (m^2). The volume was based on height measurements for each of the flux measurements.

Nitrate and pH measurements. Soil samples were collected from 0–10 cm around the flux tube ($n = 3$) and kept cold at 7 °C and dark until processed in the laboratory within 3–4 days. Samples (2 g) were subsequently mixed with 10 ml deionized water and shaken for 10 min and the eluent analysed for nitrate content on standard for Ion Chromatography (Dionex Aquion, Thermo Scientific, Waltham, MA, USA) and pH values measured using a VWR pHenomenal (CO3100L).

Laboratory incubations. In-situ soil samples were taken on October 6th, 2022, on a conventional agricultural field near Sorø, Denmark, at 55°44'N, 11°59'E. Samples ($n = 40$) were collected in plastic tubes (12 cm in length, 7 cm in diameter), immediately transported to the laboratory and pre-incubated for almost four weeks at 7 °C.

Prior to drying and wetting all samples had soil water content of approximately $16.5 \pm 1.1\%$ by weight representing the ambient conditions. Nine random samples were selected for free drainage and drying. The samples were dried at room temperature for seven days. After drying for seven days, the water content was $11.3 \pm 1.3\%$. Nine other samples were wetted with deionized water 24 h prior to gas measurement to ensure completely water-filled pores and at least 2 mm standing water on top of the soil surface. The remaining nine samples represent ambient conditions.

For N-treatment, we used laboratory grade KNO₃ dissolved in deionized water to represent three levels of N input (10 kg ha⁻¹, 50 kg ha⁻¹ and 150 kg ha⁻¹). For N-treatment, we used sterile BD Plastipak 1 mL syringes to inject 10 mL of KNO₃ + H₂O in each sample. Five injections were made at 5 cm depth and 5 injections were made as the syringe was moved to the surface. From this we assume that the entire core was homogeneously treated with N. Injections were made on the 9th of November 2022.

Soil bulk density was calculated as a weight difference after complete drying at 105 °C of samples after the incubation. The content of C and N was determined on elemental analyser (CE 1110, Thermo Electron, Milan, Italy) and pH was measured in double deionized water (Silex H₂O, 1:2.5 weight to volume) and measured using a potentiometer after 3 min of calibration.

Measurements of N₂O production were conducted over eight weeks (starting 9th of November 2022) where soil samples were placed in 2 L hermetically sealed glass bottles. Between measurements samples were placed at 7 °C in a fridge open to a ventilated room but covered by parafilm (to avoid evaporation). During measurements samples were out of the refrigerator for 9 min. Room temperature was between 12 and 17 °C. From each bottle, two Versilon SE200 tubes of 120 cm were connected to an isotopic N₂O-analyser. On the inlet tube a 0.1 mm Whatman paper filter was attached. Luer lock “fittings” were attached to the end. Gas was continuously sampled using Isotopic N₂O Analyser, 914-0027, from Los Gatos Research (Quebec, Canada), with a flow rate of 143 mL min⁻¹, and specific volume of 50 cm³. The analyser logged N₂O in ppm at 1 Hz frequency, each measurement was 8 min. Each sample was measured daily for 17 days, then every second day for seven days and then twice a week until week 10.

The first 200 s of each measurement was discarded as the analyser needed time to mix up residue air and sample from the bottle. Final N₂O fluxes were calculated similarly as described for field measurements.

Data availability

All data sets are available at University of Copenhagen - Electronic Research Data Archive (UCPH ERDA): <https://sid.erd.dk/sharelink/aVLxzkLNP3>.

Received: 13 May 2023; Accepted: 9 November 2023;

Published online: 08 December 2023

References

1. IPCC: Climate Change 2021: The Physical Science Basis. Contribution of Working Group I to the Sixth Assessment Report of the Intergovernmental Panel on Climate Change [Masson-Delmotte, V., et al (eds.)]. Cambridge University Press, Cambridge, United Kingdom and New York, NY, USA, 2391 (2021).
2. Thompson, R. L. et al. Acceleration of global N₂O emissions seen from two decades of atmospheric inversion. *Nat. Clim. Change* **9**, 993–998 (2019).
3. Tian, H. et al. A comprehensive quantification of global nitrous oxide sources and sinks. *Nature* **586**, 248–256 (2020).
4. Butterbach-Bahl, K., Baggs, E. M., Dannenmann, M., Kiese, R. & Zechmeister-Boltenstern, S. Nitrous oxide emissions from soils: How well do we understand the processes and their controls? *Philos. Trans. R. Soc.: Biol. Sci.* **368**, 20130122 (2013).
5. Jørgensen, C. J., Struwe, S. & Elberling, B. Temporal trends in N₂O flux dynamics in a Danish wetland – effects of plant-mediated gas transport of N₂O and O₂ following changes in water level. *Global Change Biol.* **18**, 210–222 (2012).
6. Harris, E. et al. Denitrifying pathways dominate nitrous oxide emissions from managed grassland during drought and rewetting. *Sci. Adv.* **7**, eabb7118 (2021).
7. Lawrence, N. C., Tenesaca, C. G., VanLoocke, A. & Hall, S. J. Nitrous oxide emissions from agricultural soils challenge climate sustainability and in the US Corn Belt. *Proc. Natl. Acad. Sci.* **118**, e2112108118 (2021).
8. Roy, E. D., Hammond Wagner, C. R. & Niles, M. T. Hot spots of opportunity for improved cropland nitrogen management across the United States. *Environ. Res. Lett.* **16**, 035004 (2021).
9. Russell, E. S. et al. N₂O emissions from two agroecosystems: High spatial variability and long pulses observed using static chambers and the flux-gradient technique. *J. Geophys. Res.* **124**, 1887–1904 (2019).
10. Sandersen, P. B. E. A basic geological complexity map for use in the implementation of the MapField concept. Geological Survey of Denmark and Greenland Report 2021/37 (2021). https://mapfield.dk/Media/637602161172274893/GEUS_report_2021_37_A%20basic%20geological%20complexity%20map_MapField.pdf.

11. Hansen, B. et al. Assessment of complex subsurface redox structures for sustainable development of agriculture and the environment. *Environ. Res. Lett.* **16**, 025007 (2021).
12. Kim, H. et al. A 3D hydrogeochemistry model of nitrate transport and fate in a glacial sediment catchment: A first step toward a numerical model. *Sci. Total Environ.* **776**, 146041 (2021).
13. Nielsen, O.-K. et al. Denmark's National Inventory Report 2022 (494). Scientific Report from DCE <http://dce2.au.dk/pub/SR494.pdf> (2022).
14. Wallman, M. et al. Nitrous oxide emissions from five fertilizer treatments during one year – High-frequency measurements on a Swedish Cambisol. *Agric. Ecosyst. Environ.* **337**, 108062 (2022).
15. Pärn, J. et al. Nitrogen-rich organic soils under warm well-drained conditions are global nitrous oxide emission hotspots. *Nat. Commun.* **9**, 1135 (2018).
16. Lienggaard, L. et al. Extreme emission of N₂O from tropical wetland soil (Pantanal, South America). *Front. Microbiol.* **3**, 433 (2013).
17. Ambus, P. & Christensen, S. Spatial and seasonal nitrous oxide and methane fluxes in Danish forest-, grassland-, and agroecosystems. *J. Environ. Qual.* **24**, 993–1001 (1995).
18. Schelde, K. et al. Spatial and temporal variability of nitrous oxide emissions in a mixed farming landscape of Denmark. *Biogeosciences* **9**, 2989–3002 (2012).
19. Wagner-Riddle, C., Bagges, E. M., Clough, T. J., Fuchs, K. & Petersen, S. O. Mitigation of nitrous oxide emissions in the context of nitrogen loss reduction from agroecosystems: managing hot spots and hot moments. *Curr. Opin. Environ. Sustain.* **47**, 46–53 (2020).
20. Pettersen, R. J., Blicher-Mathiesen, G., Rolighed, J., Andersen, H. E. & Kronvang, B. Three decades of regulation of agricultural nitrogen loads: Experiences from the danish agricultural monitoring program. *Sci. Total Environ.* **787**, 147619 (2021).
21. Adhikari, K., Minasny, B., Greve, M. B. & Greve, M. H. Constructing a soil class map of Denmark based on the FAO legend using digital techniques. *Geoderma* **214–215**, 101–113 (2014).
22. Cappelen, J. (ed), other contributors C. Kern-Hansen, E. V. Laursen, P. Viskum Jørgensen & B. V. Jørgensen. DMI Report 21-02 Title Denmark – DMI Historical Climate Data Collection 1768-2020. Danish Meteorological Institute. <https://www.dmi.dk/fileadmin/Rapporter/2021/DMIREp21-02.pdf> (2021).
23. Kim, D.-G., Hernandez-Ramirez, G. & Giltrap, D. Linear and nonlinear dependency of direct nitrous oxide emissions on fertilizer nitrogen input: A meta-analysis. *Agric. Ecosyst. Environ.* **168**, 53–65 (2013).
24. Del Grosso, S. J. et al. A gap in nitrous oxide emission reporting complicates long-term climate mitigation. *Proc. Natl. Acad. Sci.* **119**, e2200354119 (2022).
25. Baral K. R., Jayasundara S., Brown S. E. & Wagner-Riddle, C. Long-term variability in N₂O emissions and emission factors for corn and soybeans induced by weather and management at a cold climate site. *Sci. Total Environ.* **815**, 152744 (2022).
26. Gregersen, I. B. et al. Long term variations of extreme rainfall in Denmark and southern Sweden. *Clim. Dyn.* **44**, 3155–3169 (2015).
27. Sigler, W. A. et al. Water and nitrate loss from dryland agricultural soils is controlled by management, soils, and weather. *Agric. Ecosyst. Environ.* **304**, 107158 (2020).
28. Stewart, K. J., Grogan, P., Coxson, D. S. & Siciliano, S. D. J. Topography as a key factor driving atmospheric nitrogen exchanges in arctic terrestrial ecosystems. *Soil Biol. Biochem.* **70**, 96–112 (2014).
29. Suriyavirun, N., Krichels, A. H., Kent, A. D. & Yang, W. H. Microtopographic differences in soil properties and microbial community composition at the field scale. *Soil Biol. Biochem.* **131**, 71–80 (2019).
30. Wu, L. et al. Increased N₂O emission due to paddy soil drainage is regulated by carbon and nitrogen availability. *Geoderma* **432**, 116422 (2023).
31. O. Ronneberger, P. Fischer, and T. Brox, “U-Net: Convolutional Networks for Biomedical Image Segmentation,” in Medical Image Computing and Computer-Assisted Intervention – MICCAI 2015, Cham, **2015**, 234–241 (2015).
32. Mishra, V., Limaye, A. S., Muench, R. E., Cherrington, E. A. & Markert, K. N. Evaluating the performance of high-resolution satellite imagery in detecting ephemeral water bodies over West Africa. *Int. J. Appl. Earth Observ. Geoinf.* **93**, 102218 (2020).
33. Kingma D. P. & Ba J. L. Adam: A method for stochastic optimization. arXiv:1412.6980v9 (2014).
34. Ioffe, S. & Szegedy, C. Batch normalization: Accelerating deep network training by reducing internal covariate shift. In *International conference on machine learning* (pp. 448–456). pmlr. (2015).
35. Agarap, A. F., Deep learning using rectified linear units (relu). arXiv preprint arXiv:1803.08375 (2018).
36. Mikołajczyk, A. & Grochowski, M. Data augmentation for improving deep learning in image classification problem. In 2018 international interdisciplinary PhD workshop (IIPhDW) (117–122). IEEE. (2018).
37. Olofsson, P. et al. Good practices for estimating area and assessing accuracy of land change. *Remote Sensing Environ.* **148**, 42–57 (2014).

Acknowledgements

This work is funded by The Danish National Research Foundation (CENPERM DNR100) and the Pioneer Centre for Landscape Research in Sustainable Agricultural Futures (Land-CRAFT). Additional support came from two additional projects funded by the Independent Research Fund Denmark “Limiting N₂O emission from hot spots in Danish agricultural soils—linking crop roots and nitrate dynamics to develop new strategies to mitigate trace gasses” and “UV-stimulated nitrous oxide emissions, the ignored impact on atmospheric warming (UVwarm)”. Many thanks to farmers for allowing the work on private fields and to journal reviewers for very constructive revision comments.

Author contributions

The study was conceived and designed by B.E., data collected by B.E., H.F.E.H. and G.M.K., analysis made by B.E., H.F.E.H., G.M.K., P.A., X.T. and D.G., B.E. wrote the paper and benefitted from discussions and comments from all co-authors.

Competing interests

The authors declare no competing interests.

Additional information

Supplementary information The online version contains supplementary material available at <https://doi.org/10.1038/s43247-023-01095-8>.

Correspondence and requests for materials should be addressed to By Bo Elberling.

Peer review information *Communications Earth & Environment* thanks Jaan Parn and the other, anonymous, reviewer(s) for their contribution to the peer review of this work. Primary Handling Editors: Huai Chen and Clare Davis. Peer reviewer reports are available.

Reprints and permission information is available at <http://www.nature.com/reprints>

Publisher's note Springer Nature remains neutral with regard to jurisdictional claims in published maps and institutional affiliations.



Open Access This article is licensed under a Creative Commons Attribution 4.0 International License, which permits use, sharing, adaptation, distribution and reproduction in any medium or format, as long as you give appropriate credit to the original author(s) and the source, provide a link to the Creative Commons license, and indicate if changes were made. The images or other third party material in this article are included in the article's Creative Commons license, unless indicated otherwise in a credit line to the material. If material is not included in the article's Creative Commons license and your intended use is not permitted by statutory regulation or exceeds the permitted use, you will need to obtain permission directly from the copyright holder. To view a copy of this license, visit <http://creativecommons.org/licenses/by/4.0/>.

© The Author(s) 2023